

# Tuning of Catalytic Activity by Thermoelectric Materials for Carbon Dioxide Hydrogenation

Abdenour Achour, Kan Chen, Michael J. Reece, and Zhaorong Huang\*

An innovative use of a thermoelectric material (BiCuSeO) as a support and promoter of catalysis for CO<sub>2</sub> hydrogenation is reported here. It is proposed that the capability of thermoelectric materials to shift the Fermi level and work function of a catalyst lead to an exponential increase of catalytic activity for catalyst particles deposited on its surface. Experimental results show that the CO<sub>2</sub> conversion and CO selectivity are increased significantly by a thermoelectric Seebeck voltage. This suggests that the thermoelectric effect can not only increase the reaction rate but also change chemical equilibrium, which leads to the change of thermodynamic equilibrium for the conversion of CO<sub>2</sub> into hydrogenation reactions. It is also shown that this thermoelectric promotion of catalysis enables BiCuSeO oxide itself to have a high catalytic activity for CO hydrogenation. The generic nature of the mechanism suggests the possibility that many catalytic chemical reactions can be tuned in situ to achieve much higher reaction rates, or at lower temperatures, or have better desired selectivity through changing the backside temperature of the thermoelectric support.

T absolute temperature<sup>[1]</sup> Most currently used TE materials are heavy-metal-based, such as Bi<sub>2</sub>Te<sub>3</sub> and PbTe, due to their high ZT. However, these materials are not best suited for medium to high temperature, large scale applications, because of problems such as their low melting, or decomposition, or oxidation temperatures. They are also harmful to environment and contain scarce constituent elements. On the other hand, oxide TE materials, such as p-type layered BiCuSeO, cobalt oxide A<sub>x</sub>CoO<sub>2</sub> (A = Na, Ca, Sr), and n-type NaTaO<sub>3</sub>-Fe<sub>2</sub>O<sub>3</sub>, CaMnO<sub>3</sub> and SrTiO<sub>3</sub> based perovskites, can overcome these disadvantages.<sup>[2]</sup> TE devices are usually configured in modules by connecting the p-type and n-type TE legs electrically in series and thermally in parallel. We report here an innovative use of TE materials as a catalyst support and show its substantial promotional effect on catalytic activity. BiCuSeO (BCSO) was selected as the thermoelectric materials for this investigation because it possesses good TE properties to over 900 K, an extraordinary low intrinsic thermal conductivity of less than 0.5 W m<sup>-1</sup> K<sup>-1</sup>; therefore, a high temperature difference can easily built up across this material; high Seebeck coefficient up to 500 V K<sup>-1</sup> at room temperature and greater than 300 V K<sup>-1</sup> at high temperatures, and no decomposition below 773 K.

## 1. Introduction

Thermoelectric (TE) materials have recently attracted wide-spread interest in research because they can convert a temperature difference directly into an electrical voltage via the Seebeck effect,  $S = V/T$ , where  $V$  is the voltage between the two ends of the TE material and  $T$  the temperature difference,  $S$  is the Seebeck coefficient. The performance of a TE material is ranked by its figure of merit  $ZT = S^2$ .

Catalyst promoters improve the activity, selectivity, or lifetime of a catalyst and can generally be divided into structural and electronic promoters. Structural promoters enhance and stabilize the dispersion of the catalyst on the support. Electronic promoters induce changes of electronic state of the catalyst near the Fermi level.<sup>[3]</sup> These promoters are added and mixed during the catalyst preparation and therefore can be subject to degradation during the catalytic process. On the other hand, electrochemical promotion, also called non-Faradaic electrochemical modification of catalytic activity (NEMCA), which allows for controlled in situ introduction of promoters on catalyst surfaces under operating conditions.<sup>[3,4]</sup> NEMCA has proved to be an excellent research technique but its large scale industrial use has been limited due to its shortcomings: (i) low efficiency of catalyst materials (which are often expensive noble metals) because it requires a continuous electrode to maintain conductivity, (ii) need to maintain electrical connection under often harsh conditions, and (iii) the incompatibility of its reactor configuration (often a fuel cell configuration) with typical chemical reactors (fixed bed, monolithic, and fluidized bed).<sup>[5]</sup>

We report here the realization of in situ, reversible, and significant modification of catalytic activity for both continuous

A. Achour, Dr. Z. Huang  
Surface Engineering and Nanotechnology Institute  
Cranfield University  
Bedfordshire MK43 0AL, UK  
E-mail: z.huang@cranfield.ac.uk

Dr. K. Chen, Prof. M. J. Reece  
School of Engineering and Materials Science  
Queen Mary  
University of London  
Mile End Rd, London E1 4NS, UK

 The ORCID identification number(s) for the author(s) of this article can be found under <https://doi.org/10.1002/aenm.201701430>.







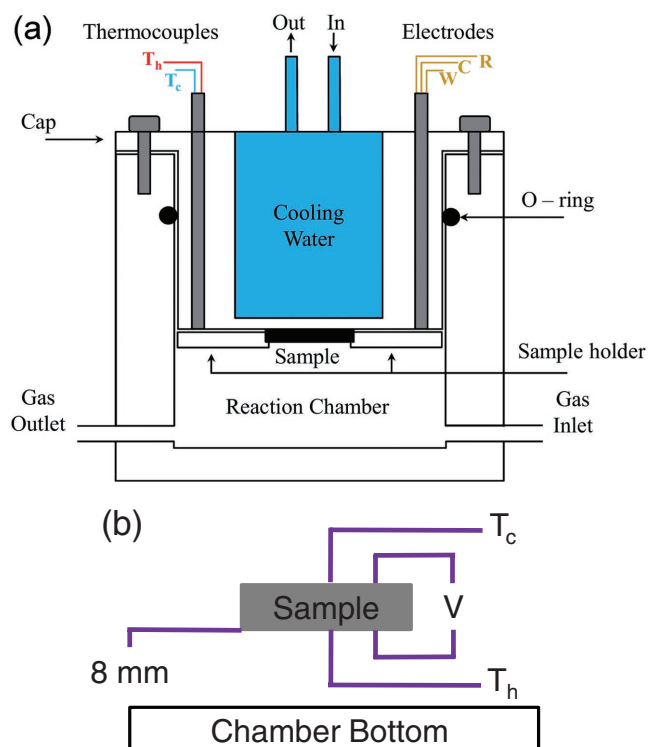


Figure 4. a) Schematic diagram of the single chamber reactor which can combine thermoelectric effect with catalytic chemical reaction. b) Schematic diagram of the arrangement of the sample and the measured parameters for all the catalytic reaction experiments.  $T_h$  and  $T_c$  were measured temperatures at the top and bottom surfaces of the sample, and  $V$  the corresponding Seebeck voltage. The bottom surface of the sample was about 8 mm above the bottom of the stainless steel chamber. The temperature of the chamber bottom was 200–300 K higher than the bottom of the disc sample.

surface  $T_c$  (nominal surface area 100 mm<sup>2</sup>), and the side wall of the disc (nominal surface area 40 mm<sup>2</sup>) sample. From Tables S1 and S2 (Supporting Information), it can be seen that when  $T_h$  was below 403 K no CO<sub>2</sub> conversion was obtained, and  $T_c$  was never higher than 331 K. Especially at high temperatures,  $T_h$  was much higher than  $T_c$ , and the temperature of the side wall was between  $T_c$  and  $T_h$ . For these reasons we assume that for all of the samples, the measured CO<sub>2</sub> conversion rate was contributed from the hot surface  $T_h$  only, and the contributions from the cold surface  $T_c$  and the side wall of the disc sample were negligible.

### 3.3.2. Higher Catalytic Activity at the Same Temperature under TE than RTE Conditions

The reaction products observed were only CO and CH<sub>4</sub> with the vast majority (90%) being CO (Figure 5a). Figure 5b shows the CO<sub>2</sub> conversion as a function of temperature  $T_h$  under the TE and RTE conditions for Pt(80)/BCSO and BCSO with a inlet gas ratio of CO/H<sub>2</sub> = 1:1. It can be seen that for the same sample at the same temperature, the CO<sub>2</sub> conversion  $X$  under TE conditions was much greater than under RTE conditions. For example, for Pt(80)/BCSO at 573 K, the CO<sub>2</sub> conversion

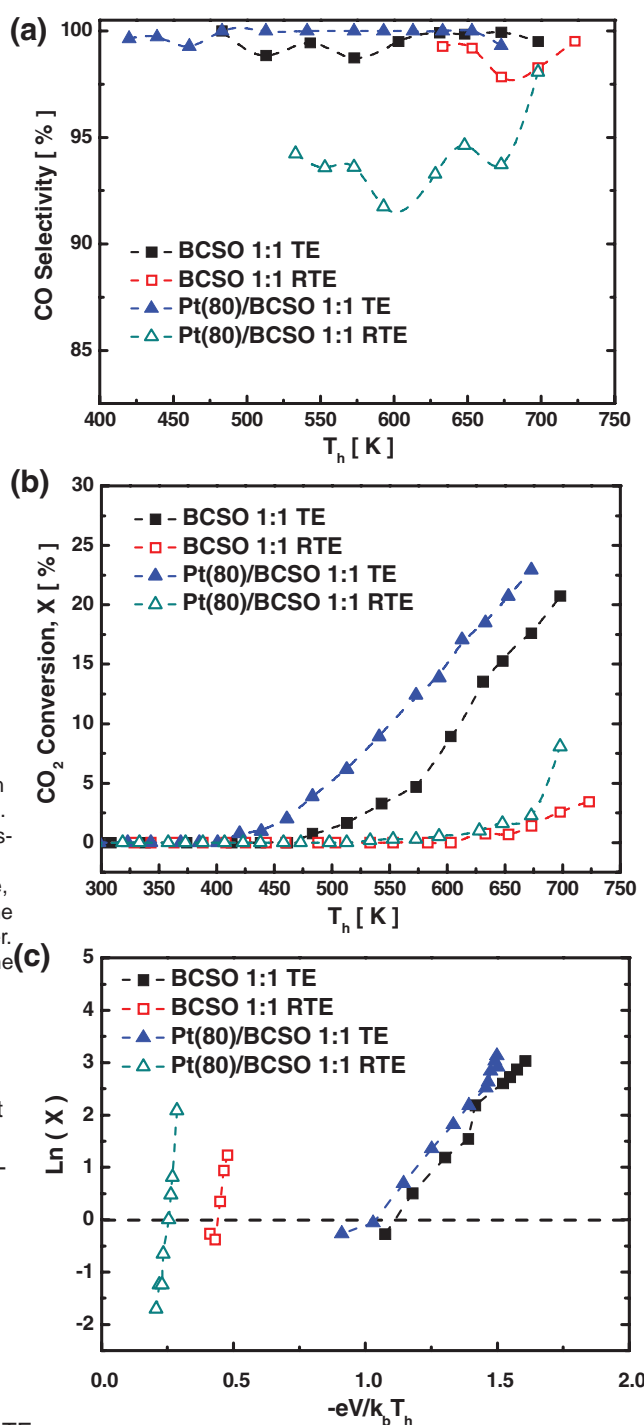


Figure 5. a) CO selectivity and b) CO<sub>2</sub> conversion  $X$  for Pt(80)/BCSO and bare BCSO with inlet gas ratio CO/H<sub>2</sub> = 1:1. For the same sample at the same temperature  $T_h$ , the conversion under large temperature gradient TE conditions was at least 10 times higher than under reduced temperature gradient RTE conditions c) a linear relationship exists between  $\ln(X)$  and  $eV/k_b T_h$ .

under TE condition was 12.4%, 42 times higher than 0.3% under RTE conditions. At 673 K, the CO<sub>2</sub> conversion under TE condition was 10 times higher than under RTE conditions. Also, CO<sub>2</sub> conversion (0.8%) was first obtained at 420 K under

the TE conditions, much lower than 553 K when it was first measured under the RTE conditions (0.2%). It is plausible to assume that relative to conditions without any TE effect, the promotional effect should be even higher. It is worthy to point out that similar experiments were repeated at least once and the results were reproducible (the same samples were used for inlet gas compositions, all under TE conditions. Figure 6a displays the measured thermoelectric voltage as a function of temperature difference  $\Delta T$  across the sample thickness for four samples, namely Pt(80)/BCSO, Pt(15)/BCSO, Pt(NP)/BCSO, and bare BCSO, at the inlet gas ratios of  $\text{CO}_2$  1:1 and 1:4. All of the four samples were weighted as 5.8 g. All of the samples had zero voltages when their bottom and top surfaces were at the same (room) temperature. The measured voltage for each sample increased linearly with temperature difference. The linear gradient for Pt(80)/BCSO was 319  $\text{V/K}$  at  $T = 200$  K, and then decreased with increasing  $T$ . The gradients for BCSO and Pt(15)/BCSO were similar and did not change with the change of the inlet gas compositions. These are typical values for Seebeck coefficient of BCSO. Note that the first measured Seebeck coefficient of 319  $\text{V/K}$  here is lower than the  $\text{CO}_2$  conversion (0.3%) was at 493 K under TE conditions and values reported in Figure 2a for SPS processed material. The 633 K under RTE conditions (0.8%). As for Pt(80)/BCSO, at the same temperature  $T$ , the  $\text{CO}_2$  conversion under TE conditions was much higher than under RTE conditions. At 698 K, the  $\text{CO}_2$  conversion was 20.8% under TE conditions compared to 3.4% under RTE conditions. Figure 5c plots  $\ln(X)$  against  $eV/k_b T_h$  for all of the cases (for the p-type BCSO,  $V$  was negative and the term  $eV$  was positive). It can be seen that a very good linear relationship existed between  $\ln(X)$  and  $eV/k_b T_h$  obtained by changing the temperature over a smaller range (50 K over a 13 mm long sample), and generally speaking,

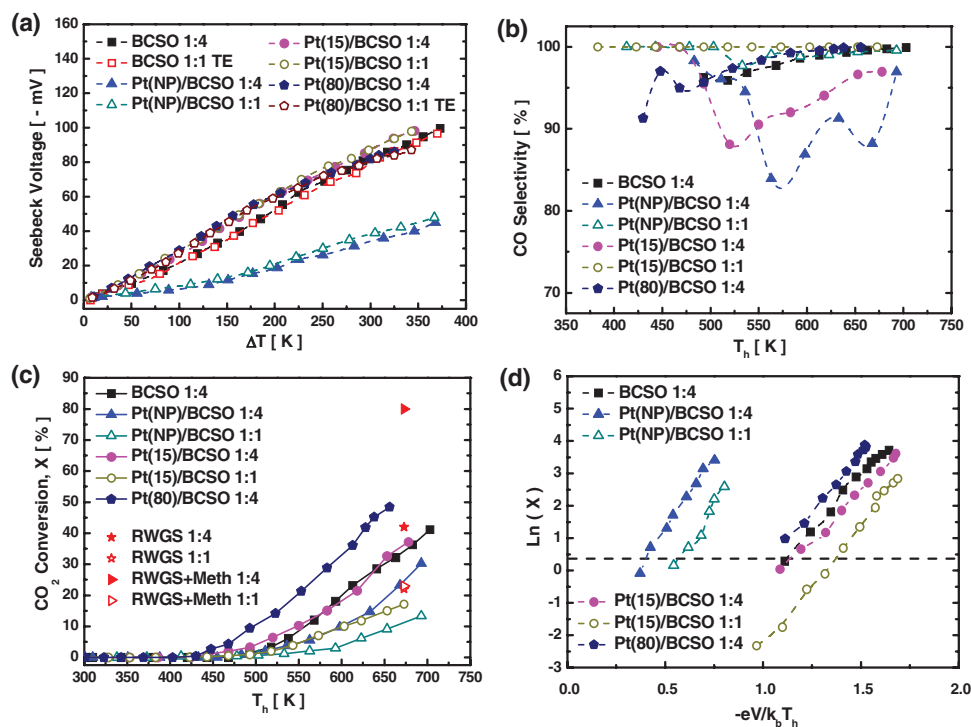


Figure 6. Thermoelectric promotion of catalytic  $\text{CO}$  hydrogenation on Pt and TE materials BCSO. a) Measured voltages as functions of temperature difference across the sample thickness. b) CO selectivity as functions of temperature. c)  $\text{CO}_2$  conversion rate  $X$  increased with temperature. d) a linear relationship exists between  $\ln(X)$  and  $eV/k_b T_h$ .

The Seebeck coefficient is temperature dependent. The  $\alpha$ -phase conversion  $X$  to be much lower than the thermal equilibrium for the Pt(NP)/BCSO was much lower, at about 136 V/rum conversion (TEC) of the reactions in Equation (1) and  $K^1$ , again, it also kept the same value when the inlet gases ratio Equation (2), so that the backward reactions were negligible. was changed from 1:1 to 1:4. This much lower Seebeck coefficient The TECs at 673 K for  $C_2O$  conversion in RWGS reaction without methanation (to CO only) are about 22% and 42% for much lower temperature (823 K as compared to 923 K for other an inlet gas ratio  $C_2O/H_2$  1:1 and 1:4 respectively; with meth-BCSO), and there were still some second phases such as  $Bi_2O_3$  and  $Bi_2O_3$  and void in the sample (Figure 3d). These results demonstrate respectively.<sup>[14,15]</sup> Under RTE conditions, the conversion rate that the measured voltage was determined by the intrinsic  $\alpha$ -phase was very low; hence, the  $C_2O$  conversion on both Pt(80)/BCSO and BCSO was far away from the TEC, so it is safe to assume the TEC only, and was not affected by the gas compositions. that the backward water-gas shift reaction can be ignored and

Again, the reaction products were found to be CO and the CO<sub>2</sub> conversion X was linearly proportional to the reaction CH<sub>4</sub>, with the majority (80%) being CO. Higher H<sub>2</sub> concentration in the inlet gases led to lower CO selectivity. The temperature dependences of CO selectivity for six cases are shown in Figure 6b, while the other two, BCSO 1:1 TE and Pt(80)/BCSO 1:1 TE, are shown in Figure 5a. Generally speaking, the CO selectivity increased with temperature and the CO conversion as a function of the hot-surface temperature T<sub>h</sub> for different samples at the inlet gas ratios of CO/H<sub>2</sub> = 1:1 or 1:4. All of the samples showed a similar trend, i.e., the conversion increased with temperature. It can be seen that for the same sample, higher H<sub>2</sub> concentration leads to higher CO conversion. Pt(80)/BCSO reached 48.4% conversion at 656 K, the highest for all of the samples, indicating that the Pt surface had the highest catalytic activity. Remarkably, even without any Pt catalyst, the TE material for BCSO (CO/H<sub>2</sub> = 1:4) itself reached a conversion of 41.2% at 703 K.

Excellent linear relationships were observed between  $\ln(X)$  with and without methanation at  $\text{CO}/\text{H}_2$  ratios 1/1 and  $\text{eV}/k_b T_h$  for all ten cases (four for Figure 5c and six for 1/4 at 673 K are also presented in Figure 6c. To the best of our knowledge, 48.4% is the highest reported CO conversion to as: 6.6 for BCSO @ 1:4 and 6.22 for BCSO @ 1:1 TE; 6.06 CO (with 100% CO selectivity) at atmosphere pressure below for Pt(15)/BCSO @ 1:4 and 7.46 for Pt(15)/BCSO @ 1:1; 673 K with an inlet gas ratio  $\text{CO}/\text{H}_2$  no larger than 4.<sup>[13,15,16]</sup> 7.2 for Pt(80)/BCSO @ 1:1 and 7.15 for Pt(80)/BCSO @ 1:4; How can the  $\text{CO}_2$  conversion to CO exceeds the TEC at 673 K? 9.09 for Pt(NP)/BCSO @ 1:4 and 9.73 for Pt(NP)/BCSO @ 1:1; It can be seen from Figure 6b that at temperatures, T 678 K, 46 for Pt(80)/BCSO @ 1:1 RTE and 25.4 for BCSO @ 1:1 RTE the CO selectivity was 95% for all the samples. Notably for Generally speaking, as can be seen from Figures 5c and 6d, Pt(80)/BCSO @ 1:4, the CO selectivity was 100% at 656 K. had similar values for all the TE conditions and much higher. The CO selectivities observed at these temperatures were also values for the RTE conditions. much higher than the predicted values under the consideration

Combining the results as shown in Figures 5c and 6d, we of thermal equilibrium.<sup>[13,15,16]</sup> These results indicate that the Seebeck voltage promoted the conversion to CO and forward

$$\ln X/X_0 = eV/k_b T_b \quad (7)$$

Here,  $X_0$  is the conversion rate where  $V$  equals zero, i.e., when  $T_c = T_h$ . For the p-type TE material BSCO,  $V$  at the surface is negative, so  $eV$  is positive and the conversion rate at the hot side  $T_h$  could be much higher with a TE voltage than without, we call this thermoelectric promotion of catalysis (TEPOC), or thermoelectrocatalysis as the TE material itself can be catalytic active. Take an experimental data point for Pt(80)/BCSO @ 1:4,  $T = 656$  K,  $V = 86$  mV, and  $\ln(X/X_0) = 7.15$ , so  $eV/k_bT_h = 10.88$ , and  $X/X_0 = 53103$ . This means that at 656 K, the conversion with a Seebeck voltage of 86 mV was more than 53 thousand times higher than without a Seebeck voltage.

RWGS reaction, and decreased the (backward) water-gas shift reaction.<sup>[15]</sup> With the assistance of an electric voltage of 1.6 kV, CO<sub>2</sub> conversion to CO on a Pt/La-ZrO catalyst reached 40.6% at 648 K, much higher than the TEC of about 20% without electric field at the same temperature.<sup>[15]</sup> This shifted the chemical equilibrium and may also be the reason why we observed the linear relationships in Figures 5c and 6d. Strictly speaking, if the conversion rate is close to the TEC of about 20% without electric field at the same temperature, the backward water-gas-shift reaction cannot be ignored, and the conversion  $X$  is not determined by the reaction rate, and Equation (4) cannot lead to Equation (7). Nevertheless, a

Equation (4) can lead to Equation (7), and vice versa, if the very good linear relationship between  $\ln(X)$  and  $eV_b/kT_h$  was observed for all the cases investigated. The most plausible



explanation is that the Seebeck voltage (or electrochemical energy  $eV$ ) shifted the reactions in Equation (1) toward the forward reaction, i.e., the RWGS against the backward water-gas shift reaction. Hence, the achieved conversion rate was still far away from the new chemical equilibrium and Equation (7) can still be explained by Equation (4).

### 3.4. Discussion

Referring to Figure 6a,c,d, all the samples, either bare BCSO or BCSO with a continuous Pt thin film Pt(80)/BCSO, or BCSO with discontinuous Pt nanoparticles Pt(15)/BCSO and Pt(NP)/BCSO, showed similar  $\text{CO}_2$  conversion dependence with the temperature  $T_h$  and Seebeck voltage  $V$  (Figures S4 and S5, Supporting Information). The four samples with similar Seebeck voltage at a particular temperature, i.e., BCSO @1:4, Pt(15)/BCSO @1:1, Pt(15)/BCSO @1:4, and Pt(80)/BCSO @1:4, also had similar  $\ln(X) = eV/k_b T_h$  relationships. The sample Pt(NP)/BCSO @ 1:1 and 1:4 had the lowest Seebeck voltage and also had a similar  $\ln(X) = eV/k_b T_h$  relationship. This suggests that the Seebeck voltage, not specific surface property, was the most important factor in determining the catalytic activity. This also agrees with the observation that the  $\text{CO}_2$  conversion dependence on the effect of the electric field than the nature of the catalyst.<sup>[15]</sup> These results also agree with the observation in NEMCA of  $\text{CO}_2$  hydrogenation in that a negative (reduced) potential increased the selectivity and reaction rate to CO, and a positive (increased) potential increased the selectivity and reaction rate to  $\text{CH}_4$ .<sup>[13,17]</sup>

From the above discussion, all the above observed results can be explained by Equation (4), i.e., the change of work function lead to the promotion of catalytic activity. This mechanism based on the change of work function through the in situ and controlled TE effect suggests that TEPOC is an effective mechanism for any metallic catalysts, regardless of their proper ties such as particle size or total amount of the metal. This is because whatever the particle size or chemisorption property, the Fermi level of the metallic particle will be the same as that of the surface TE materials supporting them. The total amount of electrons available for catalytic reaction with the increasing of the metal particles, indeed any second phase materials, will affect the TE properties such as Seebeck coefficient and electrical conductivity, as the whole system can be regarded as a TE composite. This is because all of the samples, with or without more metal Pt, are just thermoelectric materials with a different Seebeck coefficient. Of course, the metal particle surface and TE surface may have different adsorption properties, which may lead to different catalytic properties.

Since the TE effect can be realized independently of chemical reactions, its modification to the catalytic activity can be in situ under operational conditions, and controlled through the temperature, e.g., changing the water-cooling to liquid nitrogen cooling. For n-type TE materials, the Fermi level at the cold side is higher than at the hot side, but not through the formation of a double layer. the relationship  $F_{h,h} - F_{c,c} = eV$  is still valid, so is  $eV$ , but  $V$  is now positive.

The significant promotional effect of the TE effect when there is a large Seebeck voltage can be understood from the energy point of view.  $eV/k_b T_h$  can be regarded as the ratio

between the extra electrochemical energy induced by TE effect and the thermal energy of an electron at the reaction surface. At 300 K, the thermal energy  $k_b T$  is 25.9 meV. So, 104 mV of Seebeck voltage gives 104 meV extra electrochemical energy to an electron at the Fermi level, which is equivalent to the thermal energy of an electron at 1200 K, but a 104 mV Seebeck voltage can be generated by a temperature difference of 347 K by a TE material (such as BCSO) with an average Seebeck coefficient of  $300 \text{ V K}^{-1}$ . So, TE effect is a very efficient way to enhance the electrochemical energy of an electron at the reaction surface.

Considering  $eV$  in TEPOC, note that Equation (4) is similar to the rate equation for NEMCA<sup>[8,9]</sup>, which is  $\ln(r/r_0) = (A^*/k_b T) - (eV/k_b T)$ , where  $r_0$  is the open-circuit reaction rate, and  $A^*$  are empirically determined constants, is the change of work function due to the applied external voltage. Under certain conditions,  $r$  is linearly proportional to the non-Ohm drop of external potential<sup>[3,8]</sup> so the rate Equation (4) for TEPOC looks exactly the same as the rate equation for NEMCA. However, there are a few important differences between NEMCA and TEPOC. (i) No electrolyte nor external voltage are needed in the TEPOC system, while for NEMCA, an electrical insulating electrolyte layer is crucial otherwise a non-Ohm drop of potential (or ionic current) cannot be established. In fact, the unusually low thermal conductivity of BCSO has been attributed to its negligible ionic conductivity, so the back spill-over of ionic species in BCSO would have been negligible. Also, we did not observe any change of reaction rate when an external voltage (positive or negative) was applied to the Pt(80)/BCSO or other samples. (ii) Unlike in NEMCA, the catalyst in TEPOC (e.g., Pt) does not need to be continuous, as TE materials are electrically conductive. Highly, separately dispersed catalysts, including nanoparticle catalysts, can be promoted by TEPOC. (iii) The constant  $A^*$  in NEMCA is smaller than unity, but the values for the constant  $A^*$  in TEPOC have been found to be larger than 1. The fact that  $A^* > 1$  in the Equations (4)–(7) indicates that there is an amplification effect when chemical reactions. The mechanism for this is not clear yet, but we speculate that this is related to the increase of the number of the surface TE materials supporting them. The total amount of electrons available for catalytic reaction with the increasing of the metal particles, indeed any second phase materials, will affect the TE properties such as Seebeck coefficient and electrical conductivity, as the whole system can be regarded as a TE catalyst when there is a large Seebeck voltage. (v) Furthermore, the mechanism for the change of work function at the catalyst surface in TEPOC is different from that in NEMCA. In NEMCA, the external voltage induces the diffusion of ionic species, which form a double layer on the catalyst surface, and produce a change of the work function.<sup>[8]</sup> Hence,

## 4. Conclusions

The thermoelectric oxide BiCuSeO has been produced using a facile solid state reaction method using  $\text{Bi}_2\text{O}_3$  as a flux agent in



air. An innovative use of the thermoelectric material as a catalyst support and promoter has been proposed and investigated through the CO<sub>2</sub> hydrogenation to produce CO and CH<sub>4</sub>. A very high CO<sub>2</sub> conversion of 48.4% to CO with 100% CO selectivity under atmosphere at temperatures below 673 K with the inlet gas ratio CO<sub>2</sub>/H<sub>2</sub> = 1:4 was obtained.

It is proposed that the thermoelectric effect can change the Fermi level and therefore the work function of the electrons in the catalyst particles supported on a thermoelectric material. This change of work function leads to exponential increase of catalytic activity. It was indeed observed in experiments that the catalytic activity of metallic particles supported on the thermoelectric materials, as represented by the CO conversion, was significantly promoted by a Seebeck voltage generated through a temperature difference across the thickness of the thermoelectric support. This thermoelectric promotion of catalysis also enabled the BiCuSeO itself to possess high catalytic activity. It was further confirmed by experimental results that there exists a linear relationship between the logarithm of the catalytic activity, and  $eV/k_B T$ , which can be regarded as the ratio of extra electrochemical energy (eV) induced by thermoelectric effect and thermal energy ( $k_B T$ ) of an electron. This extra electrochemical energy can also change the chemical equilibrium and selectivity of the reaction.

The general nature of the mechanism suggests that thermoelectric promotion of catalysis could be a universal phenomenon.

**The Reaction Chamber:** Chemical reactions were performed in a single chamber reactor. A schematic diagram of the reactor can be seen in Figure 1. The cover plate was cooled with continuous running water. Gold wires (Agar Scientific, Ø 0.2 mm) were used as electrical contacts, and temperatures were measured with K-type thermocouples (Ø 0.25 mm, TC Direct) placed directly on the sample surfaces. The reaction chamber was placed directly onto a high temperature hot plate (HP99YX, Wencesco, Inc.) with a temperature controller. The Seebeck voltage was measured continuously (Figures S1 and S2, Supporting Information) between the bottom surface and the top electrode (Au) using a potentiostat–galvanostat (VersaStat 3F, Princeton Applied Research).

**Catalytic Activity Measurement:** The catalytic activity measurements of different catalysts were carried out at atmospheric pressure in a continuous flow apparatus equipped with the stainless steel reactor (Figure 1b). The reaction reactants and products were continuously monitored using online gas chromatography (GC8340, CE instruments) and online IR analyzer (G150 QGem Scientific) to quantify the concentration of H<sub>2</sub>, CO, CH<sub>4</sub>, and CO<sub>2</sub>. To monitor the temperature, a K-type thermocouple was attached (and fixed using a high temperature tape) onto the catalyst surface for the temperature measurement. Another K-type thermocouple was placed in proximity of the top surface for the temperature measurement. Carbon mass balance for all of the experiments was found to be within 6%.

The catalyst activities were investigated with the composition of carbon dioxide and hydrogen at a ratios of CO<sub>2</sub>:H<sub>2</sub> = 1:1, and CO<sub>2</sub>:H<sub>2</sub> = 1:4. All samples were tested at an overall flow rate of 100 mL min<sup>-1</sup>.

The conversion of CO<sub>2</sub> and the selectivity of CO and CH<sub>4</sub> were evaluated from the outlet carbon percentage values obtained by the gas analysis. H<sub>2</sub>O vapor was condensed before entering the GC to prevent deterioration of the GC column. CO conversion  $X_{CO_2}$ , and the selectivity of CO and CH<sub>4</sub> were calculated as

## 5. Experimental Section

**Thermoelectric Material Preparation:** The TE material BCSO was synthesized by solid-state reaction using boron oxide (99.99%, Alfa Aesar, 99%) as a flux agent in air. During the flux synthesis, the melted B<sub>2</sub>O<sub>3</sub> served as a liquid-seal on the top of the crucible. The obtained product of each sample was then ground to a fine powder. The latter was densified at 150 MPa using a hydraulic press system to form a dense pellet of 20 mm in diameter and 2 mm in thickness. Then, the green pellet was sintered at 923 K for 10 h under an argon atmosphere. Further sintering by SPS was carried out before thermoelectric property measurements, using a HP D 25/1 (FCT Systeme GmbH, Frankenblick, Germany).

**Preparation of Catalysts:** The film catalysts were deposited on BCSO by magnetron sputtering method (Nordiko). The Pt films were prepared using pure Pt (99.99%) as the sputtering target. The thicknesses of the Pt films were 80 nm for three min and 15 nm for 20 s of sputtering time, respectively named Pt(80)/BCSO and Pt(15)/BCSO. Another platinum nanoparticle sample (Pt(NP)/BCSO) was synthesized using an impregnation method. For this sample, the green pellet was calcined at 823 K for 2 h under argon atmosphere and then reduced under 5% H<sub>2</sub> in Ar at 773 K for 4 h.

The microstructural investigations were carried out using XRD (Siemens 5005) at 40 kV with a Cu K $\alpha$  source and a scanning electron microscope (Philips, FEI XL30 SFEQ).

**Thermoelectric Property Measurements:** The thermal diffusivity (D) was measured by using laser flash method (LFA-457, Netzsch, Germany) under a continuous argon flow. The total thermal conductivity ( $\kappa_{total}$ ) was calculated by the formula  $\kappa_{total} = D \rho C_p$ , where  $\rho$  was the mass density measured by the Archimedes method, while the specific heat ( $C_p$ ) was determined using a differential scanning calorimeter instrument. The electrical conductivity and Seebeck coefficient were simultaneously measured (LSR-3/1100, Linseis) in a He atmosphere.

$$CO_2 \text{ Conversion \%} = \frac{Y_{CO} + Y_{CH_4}}{Y_{CO} + Y_{CH_4} + Y_{CO_2}} \times 100 \quad (8)$$

$$CO \text{ Selectivity \%} = \frac{Y_{CO}}{Y_{CO} + Y_{CH_4}} \times 100 \quad (9)$$

$$CH_4 \text{ Selectivity \%} = \frac{Y_{CH_4}}{Y_{CO} + Y_{CH_4}} \times 100 \quad (10)$$

where  $Y_{CO_2}$ ,  $Y_{CO}$ , and  $Y_{CH_4}$  were the mol fractions of CO<sub>2</sub>, CO, and CH<sub>4</sub> in the outlet, respectively.

$X_{CO_2} = \frac{X_{CO_2} \times f_v}{22400 \times 60}$  where  $f_v$  100 mL min<sup>-1</sup> is the volumetric flow rate at the outlet of the reactor and  $r_{CO_2}$  is the CO<sub>2</sub> reaction rate.

## Supporting Information

Supporting Information is available from the Wiley Online Library or from the author.

## Acknowledgements

The work was funded by a Leverhulme Trust Research Project Grant (RPG-2013-292). Z.H. acknowledges support from the Hong Kong and Macao and Overseas Scholars Joint Research Fund of NSFC (No. 51428101) and thanks Prof. P. Peng of Hunan University, China. M.J.R. and K.C. would like to thank the Engineering and Physical Science Research Council (MASSIVE, EP/L017695/1) for its support to enable

their contribution to this work. The authors also thank Drs. C. Shaw, X. Liu, A. Stallard, and T. Pryor for technical help.

## Conflict of Interest

The authors declare no conflict of interest.

## Keywords

carbon dioxide hydrogenation, electrochemical energy, promotion of catalysis, thermoelectric materials, work function

Received May 24, 2017

Revised July 21, 2017

Published online: October 6, 2017

- [1] a) T. C. Harman, P. Taylor, M. Walsh, B. Laforge, *Science* **2002**, 297, 2229; b) K. Hsu, S. Loo, F. Guo, W. Chen, J. Dyck, C. Uher, T. Hogan, E. Polychroniadis, M. Kanatzidis, *Science* **2004**, 303, 818.
- [2] a) H. Ohta, K. Sugiura, K. Koumoto, *Inorg. Chem.* **2008**, 47, 8429; b) J. He, Y. Liu, R. Funahashi, *J. Mater. Res.* **2011**, 26, 1762; c) C. Barreateau, L. Pan, E. Amzallag, L. Zhao, D. Berardan, N. Dragoe, *Semicond. Sci. Technol.* **2014**, 29, 064001; d) C. Barreateau, D. Berardan, N. Dragoe, *J. Solid State Chem.* **2015**, 222, 53; e) L. Zhao, J. He, D. Berardan, Y. Lin, J. Li, C. Nan, N. Dragoe, *Energy Environ. Sci.* **2014**, 7, 2900; f) F. Li, T. Wei, F. Kang, J. Li, J. Alloys Compd. **2014**, 614, 394; g) W. Wunderlich, T. Mori, O. Sologub, *Mater. Renew. Sustain. Energy* **2014**, 3, 21.
- [3] C. G. Vayenas, S. Bebelis, C. Pliangos, S. Brosda, D. Tsiplakides, *Electrochemical Activation of Catalysis: Promotion, Electrochemical Promotion, and Metal-Support Interactions*, Kluwer Academic, New York 2001.
- [4] a) D. Poulidi, C. Anderson, I. Metcalfe, *Solid State Ion.* **2008**, 179, 1347; b) M. Konsolakis, N. Macleod, J. Isaac, I. Yentekakis, R. Lambert, *J. Catal.* **2000**, 193, 330; c) A. de Lucas-Consuegra, J. González-Cobos, Y. Gacia-Rodriguez, J. L. Endrino, J. L. Valverde, *Electrochem. Commun.* **2012**, 19, 55; d) A. de Lucas-Consuegra, J. González-Cobos, Y. García-Rodríguez, J. Masquera, J. L. Endrino, J. L. Valverde, *J. Catal.* **2012**, 293, 149; e) A. Kambolis, L. Lizarraga, M. Tsampas, L. Burel, M. Rieu, J. Viricelle, P. Vernoux, *Electrochem. Commun.* **2012**, 19, 5; f) I. R. Harkness, C. Hardacre, R. M. Lambert, I. V. Yentekakis, C. G. Vayenas, J. Catal. **1996**, 160, 19; g) Z. Wang, H. Huang, H. Liu, X. Zhou, *Int. J. Hydrogen Energy* **2012**, 37, 17928.
- [5] D. Tsiplakides, S. Balomenou, *Chem. Ind. Chem. Eng.* **2008**, 14, 97.
- [6] K. A. Bishop, A. M. Betzelberger, S. P. Long, E. A. Ainsworth, *Plant, Cell Environ.* **2015**, 38, 1765.
- [7] a) G. A. Olah, G. Prakash, A. Goeppert, *J. Am. Chem. Soc.* **2001**, 123, 12881; b) W. Wang, S. Wang, X. Ma, J. Gong, *Chem. Soc. Rev.* **2011**, 40, 3703; c) J. Ma, N. Sun, X. Zhang, N. Zhao, F. Xiao, W. Wei, Y. Sun, *Catal. Today* **2009**, 148, 221; d) B. Hu, C. Guild, S. Suib, *J. Catal.* **2013**, 1, 18; e) H. Jhong, S. Ma, P. Kenis, *Curr. Opin. Chem. Eng.* **2013**, 2, 191; f) G. A. Olah, *Catal. Lett.* **2004**, 1, 93; g) N. Hollingsworth, R. Taylor, M. T. Galante, J. Jacquemin, C. Longo, K. B. Holt, N. Leeuw, C. Hardacre, *Faraday Discuss.* **2015**, 183, 389.
- [8] C. G. Vayenas, S. Brosda, C. Pliangos, *J. Catal.* **2003**, 216, 487.
- [9] C. G. Vayenas, S. Bebelis, S. Ladas, *Nature* **1990**, 343, 625.
- [10] G.-K. Ren, J.-L. Lan, S. Butt, K. J. Ventura, Y.-H. Lin, C.-W. Nan, *RSC Adv.* **2015**, 5, 69878.
- [11] J. Li, J. Sui, Y. Pei, X. Meng, D. Berardan, N. Dragoe, W. Cai, L.-D. Zhao, *J. Mater. Chem.* **2014**, 2, 4903.
- [12] J. Nicole, D. Tsiplakides, S. Wodiunig, Ch. Comninellis, *J. Electrochem. Soc.* **1997**, 144, L312.
- [13] E. I. Papioannou, S. Souentie, A. Hammad, C. G. Vayenas, *Catal. Today* **2009**, 146, 336.
- [14] a) A. G. Kharaji, A. Shariati, M. Ostadi, *J. Nanosci. Nanotechnol.* **2014**, 14, 1; b) R. B. Unde, *Kinetics and Reaction Engineering Aspects of Syngas Production by the Heterogeneously Catalysed Reverse Water Gas Shift Reaction*, Ph.D. Thesis, University of Bayreuth, 2012.
- [15] K. Oshima, T. Shinagawa, Y. Nogami, R. Manabe, S. Ogo, Y. Sekine, *Catal. Today* **2014**, 232, 27.
- [16] a) Y. A. Daza, J. N. Kuhn, *RSC Adv.* **2016**, 6, 49675; b) R. V. Goncalves, L. R. Vono, R. Wojcieszak, C. S. B. Dias, H. Wender, E. Teixeira-Neto, L. M. Rossi, *Appl. Catal., B* **2017**, 209, 240; c) V. Jiménez, C. Jiménez-Borja, P. Sánchez, A. Romero, E. I. Papaioannou, D. Theleritis, S. Souentie, S. Brosdac, J. Valverde, *Appl. Catal., B* **2011**, 107, 210.
- [17] a) M. Makri, A. Katsaounis, C. G. Vayenas, *Electrochim. Acta* **2015**, 179, 556; b) I. Kalaitzidou, A. Katsaounis, T. Norby, C. G. Vayenas, *J. Catal.* **2015**, 331, 98.
- [18] a) P. Vaqueiro, R. Al Orabi, S. Luu, S. Guelou, A. Powell, R. Smith, J. Song, D. Wee, M. Fornari, *Phys. Chem. Chem. Phys.* **2015**, 17, 31735; b) L. Zhao, J. Li, in *BiCuSeO: A Promising Thermoelectric Material*, in *Materials Aspect of Thermoelectricity* (Ed. C. Uher), CRC Press, Boca Raton, FL 2016.
- [19] I. Metcalfe, *J. Catal.* **2001**, 199, 259.

2017-10-06

# Tuning of catalytic activity by thermoelectric materials for carbon dioxide hydrogenation

Achour, Abdenour

Wiley

---

Achour A, Chen K, Reece MJ, Huang Z. (2018) Tuning of catalytic activity by thermoelectric materials for carbon dioxide hydrogenation. *Advanced Energy Materials*, Volume 8, Issue 5, February 2018, Article number 1701430

<http://dx.doi.org/10.1002/aenm.201701430>

Downloaded from Cranfield Library Services E-Repository